Electronic Supplementary Information

Stereoisomers of Natural Flavonoid Exhibit Different Disruptive Effect and Mechanism of Action on $A\beta_{42}$ Protofibril

Chendi Zhan,[a] Zenghui Lao,[a] Yiming Tang,[a] Qin Qiao[b] and Guanghong Wei * [a]

[a]Department of Physics, State Key Laboratory of Surface Physics, and Key Laboratory for Computational Physical Sciences (Ministry of Education), Fudan University, Shanghai 200438, People's Republic of China.
[b]Digital Medical Research Center, School of Basic Medical Sciences, Shanghai Key Laboratory of Medical Imaging Computing and Computer Assisted Intervention, Fudan University, Shanghai 200032, People's Republic of China

Email: ghwei@fudan.edu.cn

There are 3 supplementary Tables and 12 supplementary Figures.

MATERIALS AND METHODS

Wild type $A\beta_{42}$ protofibril in the absence and presence of (+)-catechin ((+)-C), (-)-catechin ((-)-C) or epicatechin (EC). The initial structure of the tetrameric $A\beta_{42}$ protofibril was taken from the nanomeric fibril (pdb ID: 5OQV), which was derived using cryo-EM in combination with ssNMR data. The $A\beta_{42}$ chain (subunit) of 5OQV has an LS-shaped conformation, in which the N-terminal part (residues D1~E22) is L-shaped and the C-terminal part (residues D23~A42) is S-shaped (Fig. S1 (a)). This conformation contains three β-strand segments spanning residues 3-22 (β1), 28–35 (β2) and 41-42 (β3), and a "kink" around Y10. Three hydrophobic cores (labeled in yellow) stabilize the subunit conformation: (i) A2, F4, L34, and V36 (core1); (ii) L17, F19, and I31 (core2); (iii) A30, I32, M35, and V40 (core3). The side-chain interactions between H6/H13 and E11 stabilize the kink around Y10 (labelled in red). The salt bridges between the side chain of K28 and the COO^- group of A42 (labelled in blue) at the C-terminal contribute to the stability of the subunit conformation. $A\beta_{42}$ protofibril in the presence of (+)-catechin ((+)-C), (-)-catechin ((-)-C) and epicatechin (EC) were simulated. The molar ratio of flavonoids to $A\beta_{42}$ chains is 5:1, following the previous experiments, which reported that at this molar concentration, catechin and epicatechin had the best inhibitory effect on Aβ induced cytotoxicity[1]. Initial structures of $A\beta_{42}$+(+)-C, $A\beta_{42}$+(-)-C and $A\beta_{42}$+EC

systems are illustrated respectively in Fig. S1 (b), (c) and (d). The structures, partial charges, and bonded parameters (including the rotational parameters) are all obtained through a standard procedure used by many research groups[1-6]. The 3D structures of (+)-C, (-)-C and EC (Fig.1) were taken from PubChem Compound Database (https://pubchem.ncbi.nlm.nih.gov/compound, (+)-C's CID=9064, (-)-C's CID =73160 and EC's CID=72276). These structures were already optimized prior to their deposition to the database. The partial charges of these three isomers are obtained by fitting to electrostatic potential calculated using the Hartree-Fock approach with the 6-31G* basis, in a way consistent with the widely-used Amber force-fields for the MD simulations of protein and nucleotide.[12, 13] Other parameters (including the rotational parameters) also obtained from the Generalized Amber Force Field (GAFF) for small molecules.[14]

Molecular Dynamics Simulations. MD simulations were performed using Gromacs 2016.4[3] on our high-performance GPU cluster. AMBER99SB-ildn force field[2] was adopted to describe the protein. The $A\beta_{42}$ protofibril was placed in the centre of cubic boxes and fully solvated with TIP3P water molecules.[4] (+)-C, (-)-C and EC molecules were randomly distributed in solution around $A\beta_{42}$ protofibril. Bond lengths within $A\beta_{42}$ protofibril and (+)-C, (-)-C and EC molecules were respectively constrained by the LINCS[5] and SETTLE[6] algorithms, allowing an integration time step of 2 fs. The Particle mesh Ewald[7] (PME) method was used to calculate the electrostatic interaction with a real-space cutoff of 1.2 nm, and the van der Waals interactions were calculated using a cutoff of 1.2 nm. The simulations were performed in the isothermal-isobaric (NPT) ensemble using periodic boundary conditions. The solute and solvent were separately coupled to an external temperature bath using a velocity rescaling method and pressure bath using the Parrinello-Rahman[8] method. The temperature and pressure were maintained at 310 K and 1 bar using coupling constants of 0.1 and 1.0 ps, respectively. Three independent MD simulations were carried out for each system. The simulation time of each MD run is 1.5 μs. A summary of all the MD simulations is given in Table S1.

Table S1: Details of MD simulations on wild type $A\beta_{42}$ protofibril (a tetramer) with and without (+)-C, (-)-C or EC.

System	Box size (nm^3)	Simulation time	Total number of atoms
$A\beta_{42}$ protofibril (pdb ID: 5OQV)	8.54×8.54×8.54	1.5 μs	61486
	7.45×7.45×7.45	1.5 μs	40755
$A\beta_{42}$: (+)-C (1:5)	7.46×7.46×7.46	1.5 μs×3	40717
$A\beta_{42}$: (-)-C (1:5)	7.44×7.44×7.44	1.5 μs×3	40672
$A\beta_{42}$: EC (1:5)	7.44×7.44×7.44	1.5 μs×3	40672

Analysis methods. The trajectory analysis was performed with our in-house codes and tools in the Gromacs 2016.4[3, 9] software package. Gromacs tools *gmx rms, gmx do_dssp*, *gmx hbond*, *gmx cluster* and *gmx mindist* were utilized to calculate the root mean square deviation (RMSD), secondary structure, hydrogen bond, the distribution of (+)-C, (-)-C and EC and salt bridge, respectively. Kink angle, contact number and $\pi-\pi$ stacking interaction were calculated by our in-house codes. In the calculation of water contact number, we only consider water molecules in the first solvation shell (within 0.35 nm) of $A\beta_{42}$ protofibril. In our study, unless specified, all the results are based on the analysis using the data from 0.5~1.5 μs. The calculation details are as follows. The structural stability of the protofibril was examined by the time evolution of RMSD of all atoms concerning the energy minimized initial structure. The influence of (+)-C, (-)-C and EC were examined by the time evolution of RMSD of all atoms for the energy minimized initial structure, the distribution of kink angle around Y10 and that of the salt bridge between K28 and A42 (K28-A42). The kink angle refers to the angle formed by two vectors, Cα (Y10) –> Cα(H6) and Cα (Y10) –> Cα(H14) (the Cα of Y10, H6 and H14 were taken as the end of the vectors). The K28-A42 salt bridge is considered to be formed when the distance between the centroids of the side-chain charged NH_3^+ group of K28 and COO^- group of A42 lie within 0.4 nm.[10] The kink angle was averaged over each chain in the protofibril. An atomic contact between (+)-C, (-)-C and EC and $A\beta_{42}$ or within $A\beta_{42}$ peptide chain was defined when two carbon atoms or a carbon atom and another heavy atom lie within 0.54 nm or any other two heavy atoms come within 0.46 nm. The residue-residue contact of two atoms from the same residue or two sequential residues was not considered. One H-bond is taken as formed if the N(O)···O(N) distance is less than 0.35 nm and the N(O)–H···O(N) angle is greater than 150°. Two aromatic rings form an aromatic interaction when their centroid distance falls within 0.65 nm. The angle between two aromatic rings was obtained by calculating the angle of the

normal vectors of the two rings. If the angle is larger than 90°, we took the supplementary angle as the angle between the two aromatic rings. The stacking patterns were roughly classified into three categories: parallel (0°−30°), herringbone (30°−60°), and perpendicular or T-shaped (60°−90°). The two-dimensional potential mean force (PMF or free energy landscape) was constructed using the relation –RT*ln[H(x, y)], where H(x, y) was the probability of a conformation having a certain value of two selected reaction coordinates, x and y. In this work, x and y refer to the centroid distance and the angle between two aromatic rings, respectively. In all the statistical analyses, the data in the first 500 ns of the 1.5 μs-MD trajectories were discarded. The Pymol[11] program was used for trajectory visualization and graphical structure analysis.

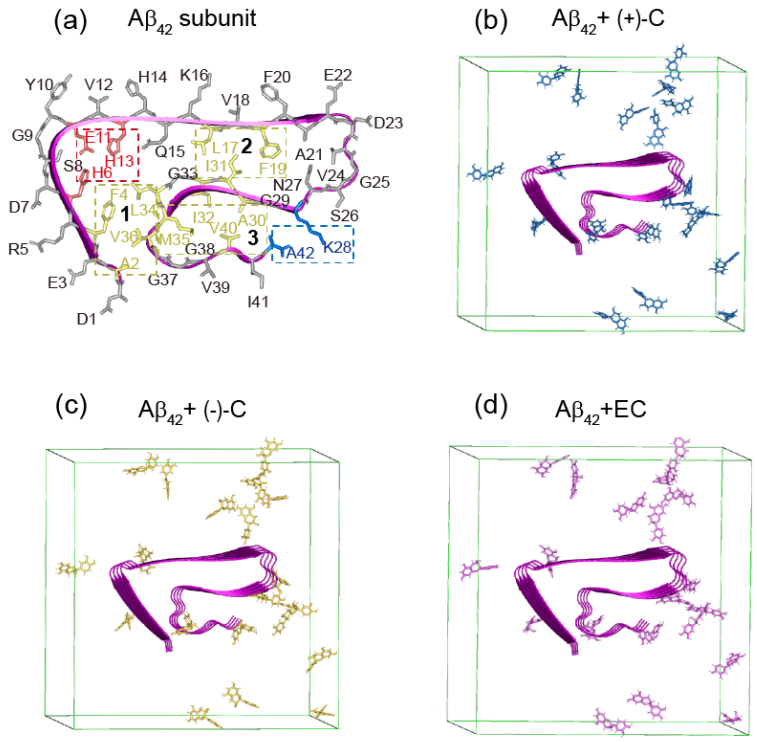

Fig. S1 The Aβ42 subunit structure and the initial simulation systems of the Aβ42 tetrameric protofibril in the presence of the 3 flavonoids. (a) The LS shaped structure of Aβ42 subunit and side-chain spatial orientation of each residue. Hydrophobic core (labelled in yellow) stabilizes the subunit conformation. The side-chain interaction between H6/H13 and E11 (labelled in red) stabilizes the kink angle around Y10. The salt bridge between K28 side chain and the COO^- group of A42 (labelled in blue) contributes to the stability of the C-terminal conformation. (b-d) The initial simulation systems of the Aβ42 tetrameric protofibril in the presence of (b) (+)-C, (c) (-)-C and (d) EC.

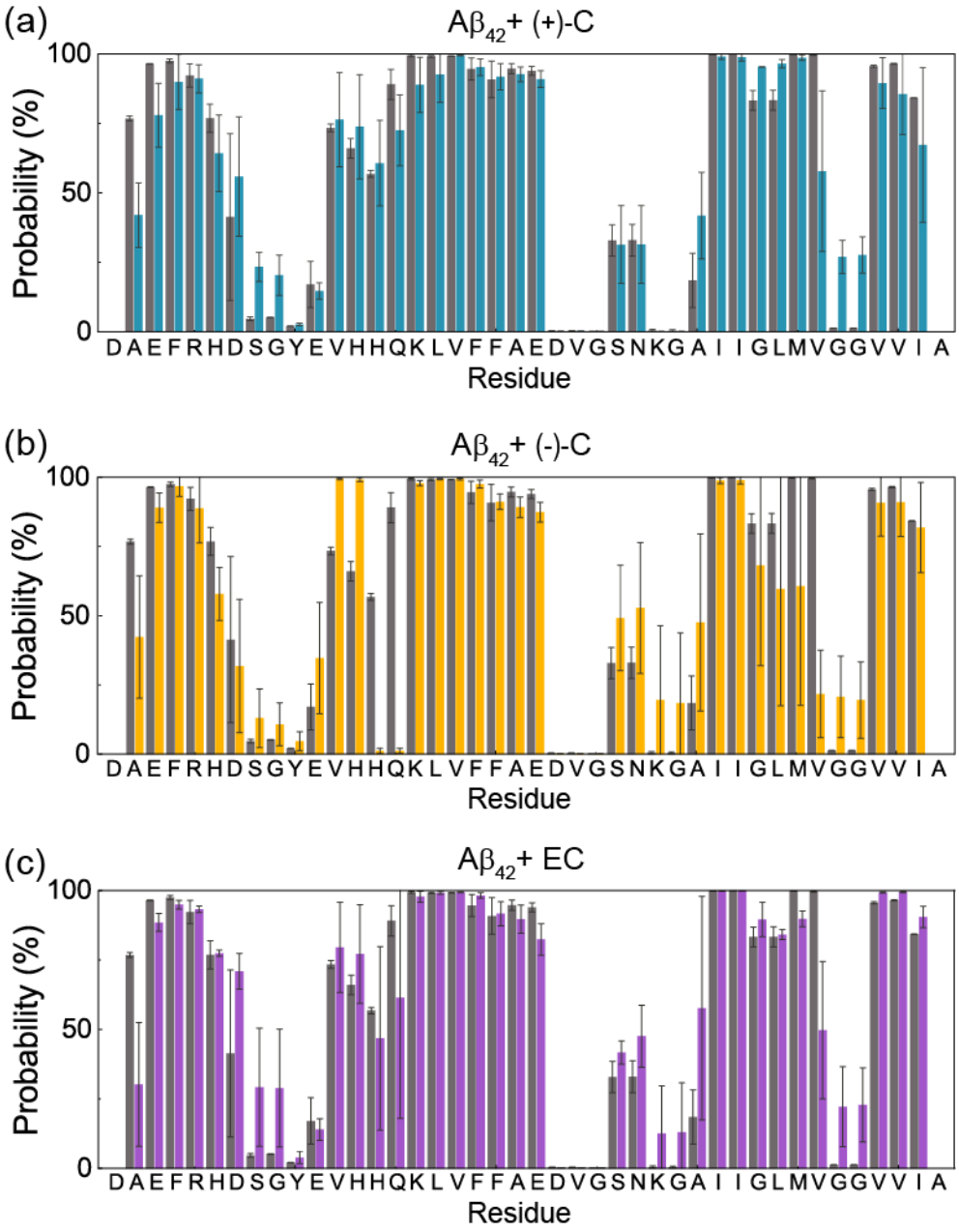

Fig. S2 Analysis of the β-sheet content of $A\beta_{42}$ protofibril. In the absence of flavonoids, theβ-sheet content of A2-D7, V12-E22, I31-V36 and V39-I41 segments are more than 50%. In the presence of (a) (+)-C, (b) (-)-C and (c) EC, the β-sheet content of these segments change in varying degrees, and (-)-C has the highest ability to decrease the β-sheet content.

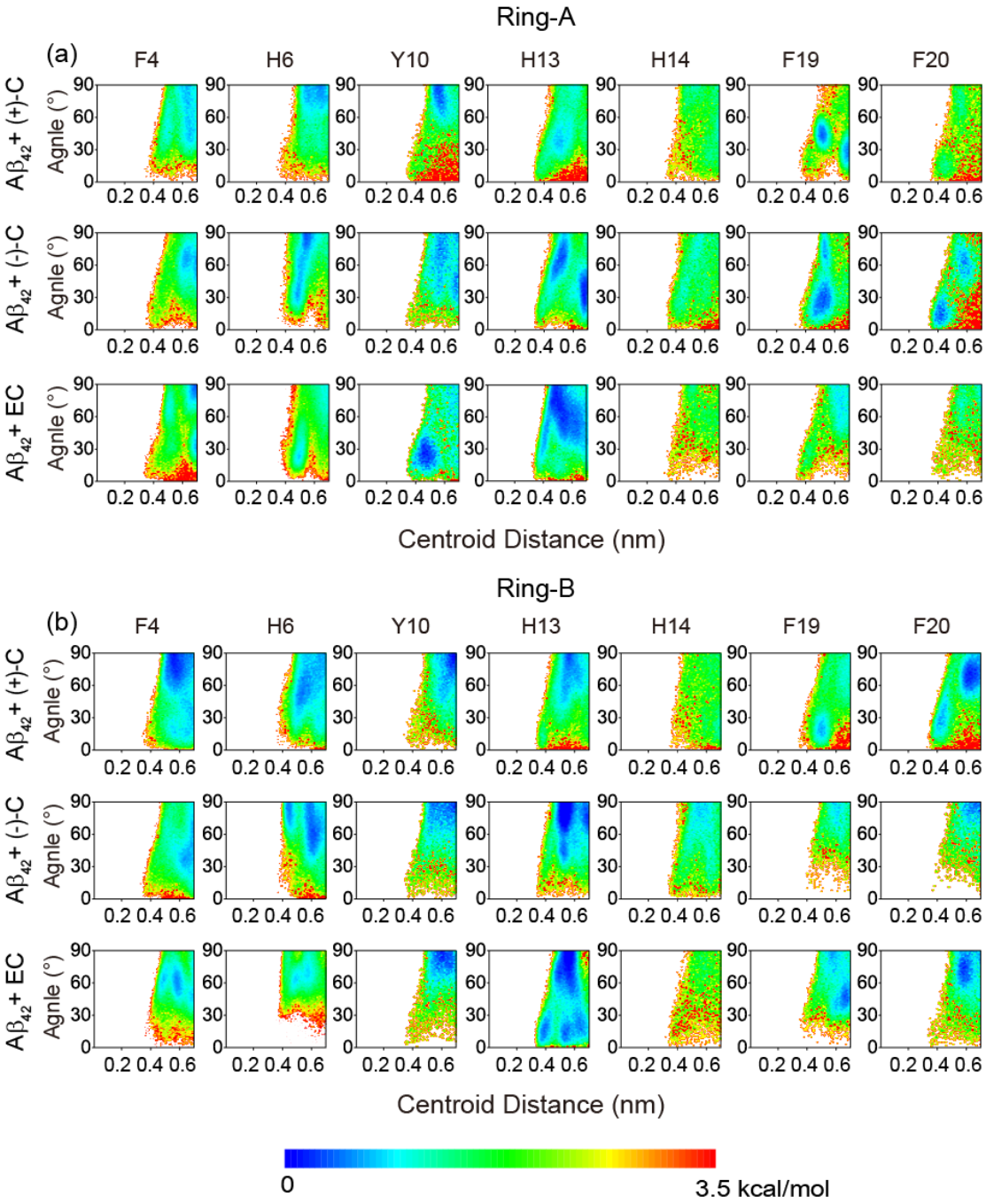

Fig. S3 Free energy landscape as a function of centroid distance and the angle between (a) Ring-A or (b) Ring-B of the three flavonoid isomers and aromatic residues of the $A\beta_{42}$ protofibril.

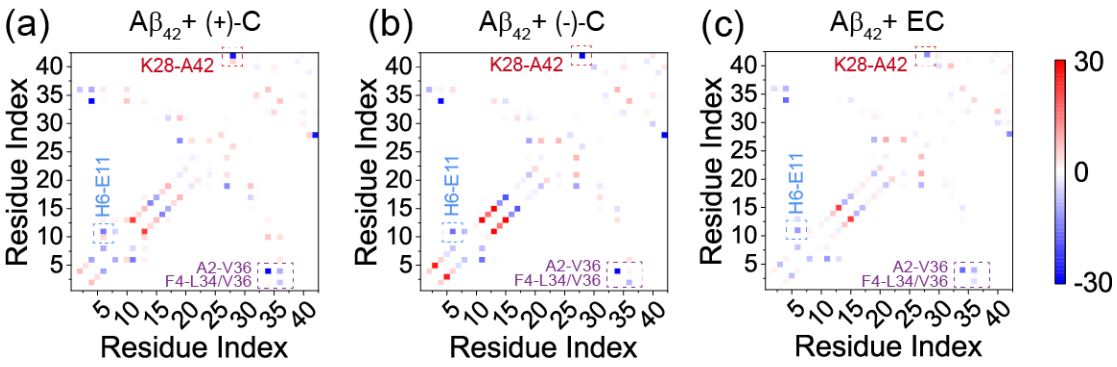

Fig. S4 Disruption of the interaction between side chains which stabilized the LS conformation by flavonoids. In the presence of (a) (+)-C, (b) (-)-C and (c) EC, the side chain interaction of a pair of residues H6-E11 is weakened, together with the attenuation of K28-A42 salt bridge and interaction among hydrophobic core 1 (A2, F4, L34 and V36) which stabilize the conformation of fibrils. (+)-C and (-)-C have a similar ability to weaken the three groups of interactions.

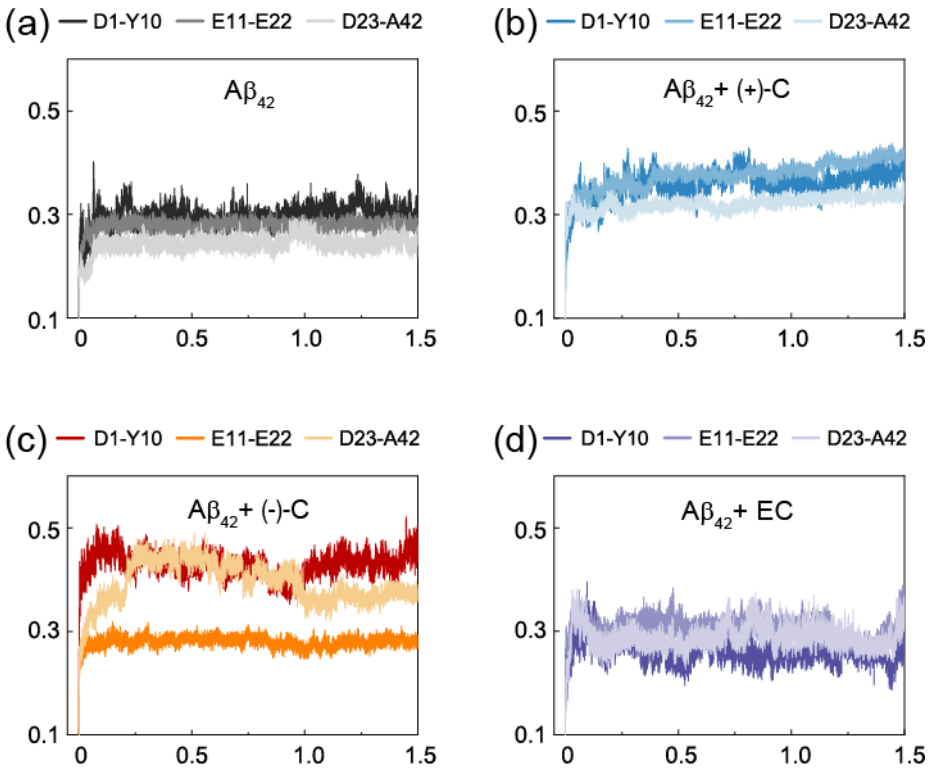

Fig. S5 The time evolved RMSD value of three segments (D1-Y10, E11-E22 and D23-A42) of $A\beta_{42}$ tetrameric protofibril in the absence (a) and presence of (b) (+)-C, (c) (-)-C and (d) EC during independent MD runs.

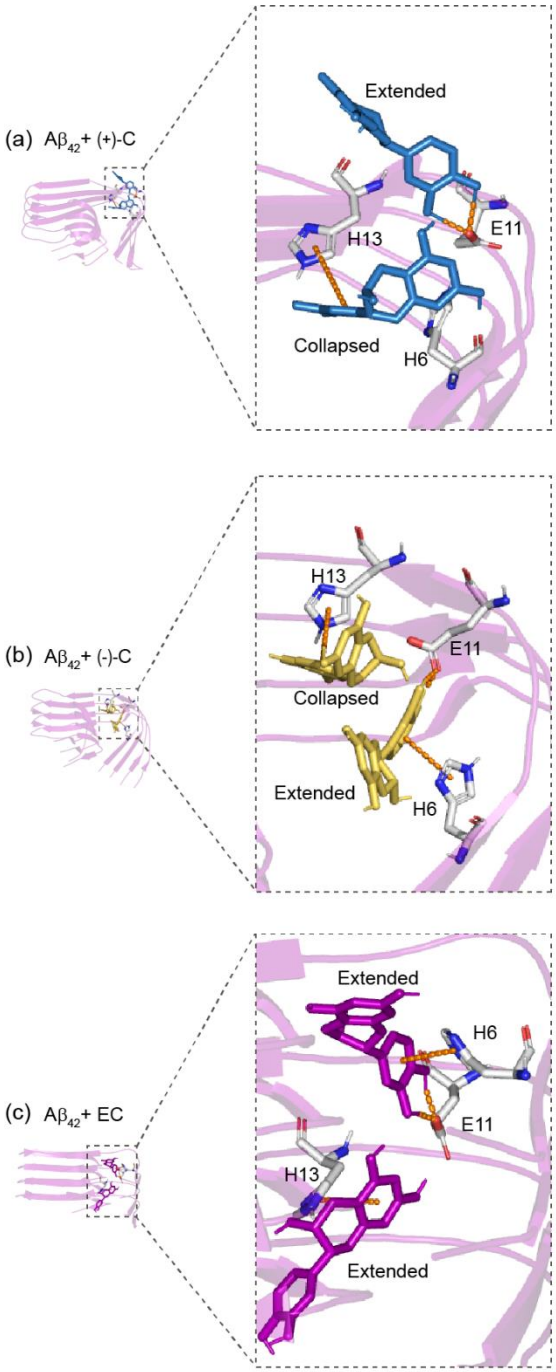

Fig. S6 Representative snapshots of the interaction between (+)-C/(-)-C and $A\beta_{42}$ protofibril. (a) The interaction between (+)-C and H6 and E11, H13. (b) The interaction between (-)-C and H6 and E11, H13. (c) The interaction between EC and H6 and E11, H13.

Table S2. The H-bond number, water-$A\beta_{42}$ and water-isomer contact numbers in each system. The numbers were calculated using the last 500 ns of each simulation trajectory.

System	$A\beta_{42}$ + (+)-C	$A\beta_{42}$ + (-)-C	$A\beta_{42}$ + EC
H-bond number	36.74±2.90	33.22±4.18	32.51±1.65
Water-$A\beta_{42}$ contact number	782.42±13.94	773.83 ±11.04	772.71±36.83
Water-isomer contact number	364.41±10.24	380.68±4.01	377.04±3.32

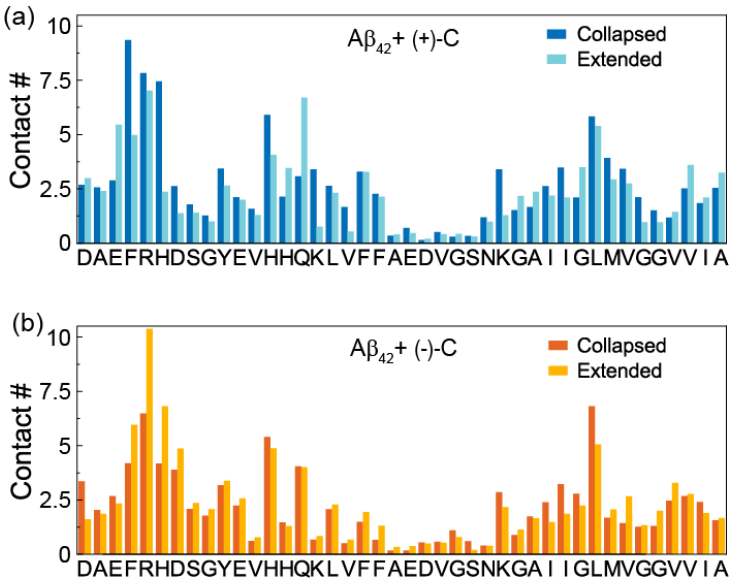

Fig. S7 Analysis of the contact number between different states of (+)-C and (-)-C and $A\beta_{42}$ protofibril. (a) The atomic contact number of the collapsed and extended state of (+)-C and each residue of $A\beta_{42}$. (b) The atomic contact number of the collapsed and extended state of (-)-C and each residue of $A\beta_{42}$.

MD simulations on mutant $A\beta_{15\text{-}40}$ protofibril in the absence and presence of (+)-catechin ((+)-C), (-)-catechin ((-)-C) or epicatechin (EC). we performed MD simulations on the Iowa mutation (D23N) of $A\beta_{15\text{-}40}$ protofibril (a tetramer) in the absence and presence of the three flavonoid isomers. The $A\beta_{15\text{-}40}$ protofibril has a U-shaped conformation (pdbID: 2MPZ).[15] The construction of the initial structure, the acquisition of parameters, the pretreatment of simulation run and the analysis methods are the same as those of isomers in wild type $A\beta_{42}$ protofibril systems. The simulation details and results are given below.

Table S3: Details of MD simulations on Iowa mutant $A\beta_{15-40}$ protofibril (a tetramer) with and without (+)-C, (-)-C or EC.

System	Box size (nm^3)	Simulation time	Number of isomers
$A\beta_{15-40}$ protofibril (pdb ID: 2MPZ)	6.45×4.73×6.22	250 ns	/
$A\beta_{15-40}$:(+)-C (1:5)	7.44×7.44×7.44	250 ns×2	20
$A\beta_{15-40}$:(-)-C (1:5)	7.44×7.44×7.44	250 ns×2	20
$A\beta_{15-40}$:EC (1:5)	7.44×7.44×7.44	250 ns×2	20

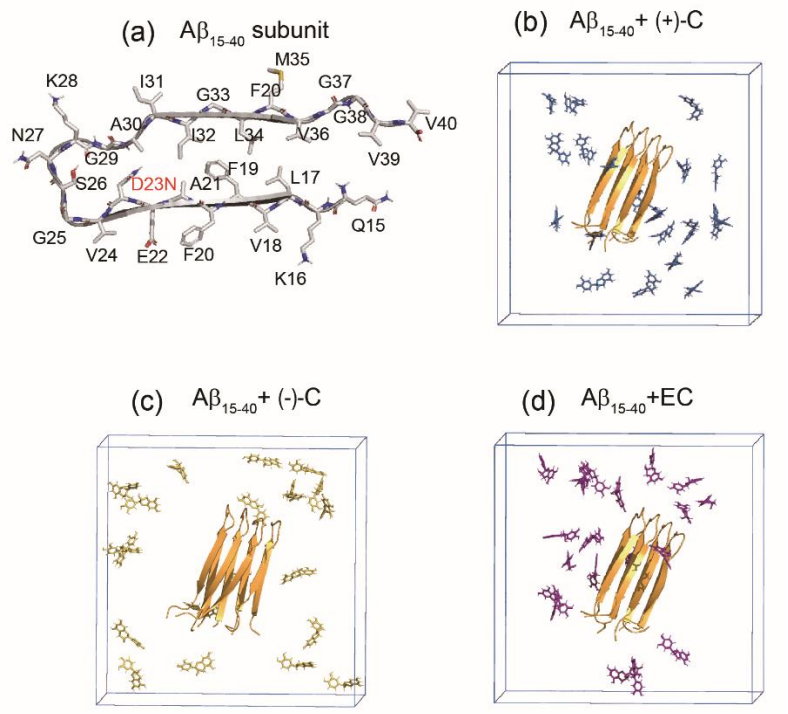

Fig. S8 The Iowa mutant (D23N) $A\beta_{15-40}$ subunit structure and the initial simulation systems of the $A\beta_{15-40}$ tetrameric protofibril in the presence of the 3 flavonoids. (a) The U-shaped structure of $A\beta_{15-40}$ subunit and side-chain spatial orientation of each residue. (b-d) The initial simulation systems of the $A\beta_{15-40}$ tetrameric protofibril in the presence of (b) (+)-C, (c) (-)-C and (d) EC.

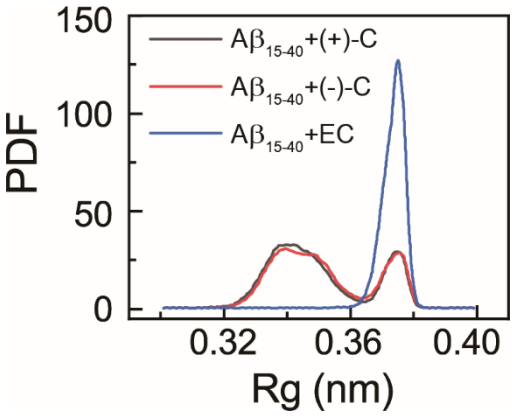

Fig. S9 The distribution of Rg of the three flavonoid isomers. (b) The distribution of Rg of (+)-C, (-)-C and EC in the $A\beta_{15-40}$ protofibril with isomers systems. (a) The distribution of Rg of a single (+)-C, (-)-C or EC molecule in water.

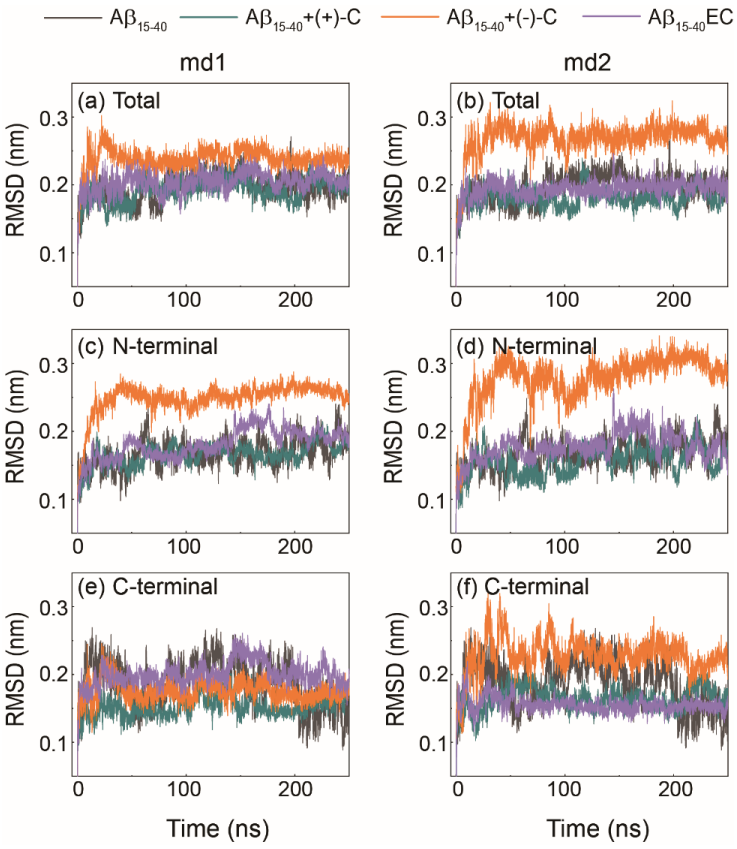

Fig. S10 The time-evolved RMSD value of $A\beta_{15-40}$ protofibril without and with (+)-C, (-)-C and EC. One MD run and two MD runs were carried out for $A\beta_{15-40}$, $A\beta_{15-40}$+(+)-C, $A\beta_{15-40}$+(-)-C and $A\beta_{15-40}$+EC systems. The all-atom RMSD value of the K18-M35 region (a, b), N-terminal (K18-V24) (c, d) and C-terminal (I31-M35) (e, f).

We first calculated the distribution of Rg of (+)-C, (-)-C and EC molecules in the three systems (Fig. S9) and found the three isomers in the mutant $A\beta_{15-40}$ protofibril systems

exhibit similar Rg distribution as those in the wild type $A\beta_{42}$ protofibril systems. The results of Rg distribution reveal that in both wild type and mutant Aβ protofibril systems, (+)-C and (-)-C mainly adopt collapsed states (with smaller Rg values) and to a lesser extent of extended states (with larger Rg values), while EC only adopts extended states. We also checked the structural stability of $A\beta_{15\text{-}40}$ protofibril in the absence and presence of (+)-C, (-)-C or EC by examining the time evolved all-atom RMSD value of the protofibril (Fig. S10). Figure S10 shows that $A\beta_{15\text{-}40}$ protofibril in the presence of (-)-C has the largest RMSD value, indicating that (-)-C displays the best protofibril-disruptive capability, especially on the N-terminal region (residues K18-V24). These results, together with the disruptive effect of the three isomers on the wild type Aβ protofibril, suggest that (-)-C has the strongest disruptive effect on both wild type and mutant Aβ protofibril. We also noted that the disruptive effect of (+)-C isomer on mutant $A\beta_{15\text{-}40}$ protofibril is less effective than on wild type one, which implies that the disruptive effect of the isomers is fibril-conformation dependent.

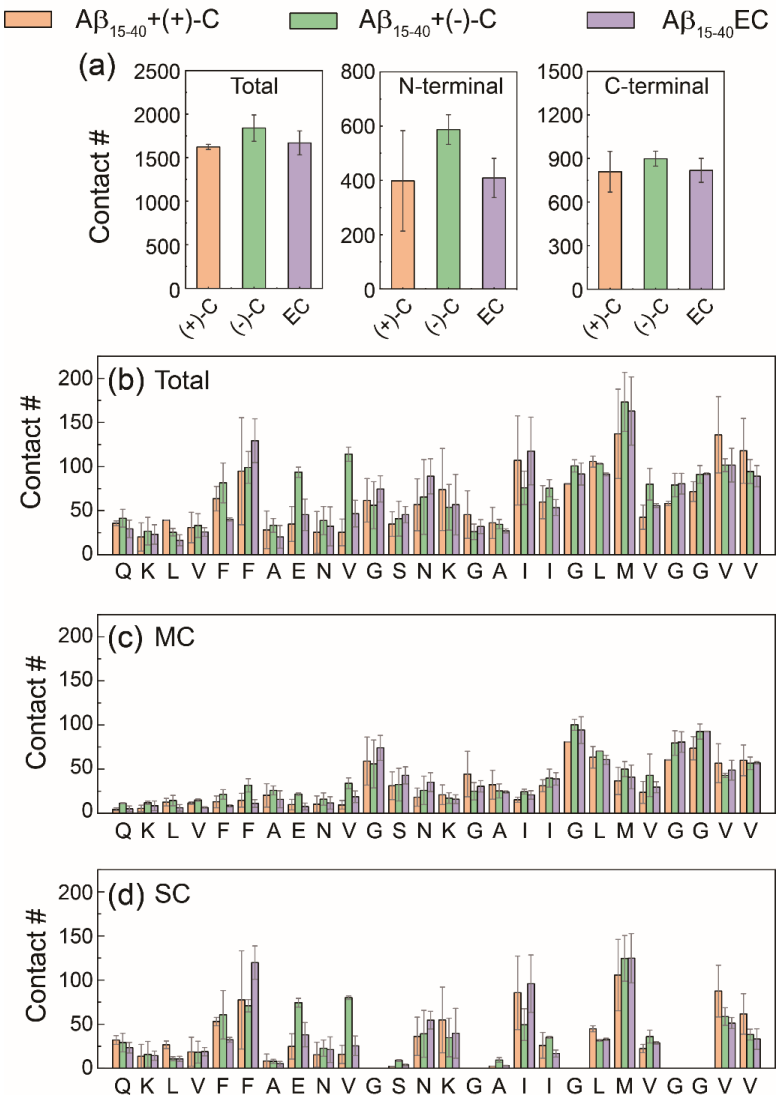

Fig. S11 Contact number analysis. (a) The total contact number between N-terminal (Q15-V24) / C-terminal (I31-V40) / all residues of $A\beta_{15\text{-}40}$ protofibril and (+)-C, (-)-C and EC. (b-d) The contact number between each residue of $A\beta_{15\text{-}40}$ protofibril and (+)-C, (-)-C and EC.

To verify whether there is a relationship between the binding modes of the three isomeric flavonoids on $A\beta_{15\text{-}40}$ protofibril and the disrupted region of $A\beta_{15\text{-}40}$, we analyzed the detailed interactions between each isomer and $A\beta_{15\text{-}40}$ protofibril. First, we calculated the contact number between N-terminal (Q15-V24) / C-terminal (I31-V40) / all residues of $A\beta_{15\text{-}40}$ protofibril and (+)-C, (-)-C and EC (Fig. S11a). It is clear that (-)-C has the largest contact number with $A\beta_{15\text{-}40}$ protofibril (right panel), especially on N-terminal (left panel). Then we calculated the contact number between each residue of $A\beta_{15\text{-}40}$ protofibril and (+)-C, (-)-C and EC (Fig. S11b-d). We found that the three isomers display similar contact numbers with $A\beta_{15\text{-}40}$, while (-)-C has the largest contact number with the main-chain of each residue of N-terminal (Q15-V24) and the side-chain of residues E22 and V24. From the above results, we concluded that among the three isomers, (-)-C has the largest contact number with the N-terminal of $A\beta_{15\text{-}40}$ protofibril, thus (-)-C has the best disruptive effect on the N-terminal.

The results reveal that the disruptive effect of the three isomers is fibril conformation-dependent. However, considering the disruptive effects on these two kinds of protofibrils, (-)-C shows the best disruptive effects, implies that (-)-C could be one of the potent drug candidates against AD.

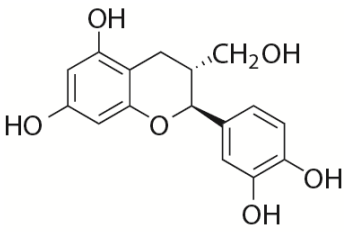

modified (+)-catechin

Fig. S12 Chemical structures of a modified (+)-C with the 3-hydroxyl group (–OH) replaced by a hydroxymethyl group ($–CH_2OH$).

References

1. H. J. Heo and C. Y. Lee, *J. Agric. Food. Chem.*, 2005, **53**, 1445-1448.
2. V. Hornak, R. Abel, A. Okur, B. Strockbine, A. Roitberg and C. Simmerling, *Proteins*, 2006, **65**, 712-725.
3. M. J. Abraham, T. Murtola, R. Schulz, S. Páll, J. C. Smith, B. Hess and E. Lindahl, *SoftwareX*, 2015, **1-2**, 19-25.

4. W. L. Jorgensen, J. Chandrasekhar, J. D. Madura, R. W. Impey and M. L. Klein, *J. Chem. Phys.*, 1983, **79**, 926-935.
5. B. Hess, H. Bekker, H. J. C. Berendsen and J. G. E. M. Fraaije, *J. Comput. Chem.*, 1997, **18**, 1463-1472.
6. S. Miyamoto and P. A. Kollman, *J. Comput. Chem.*, 1992, **13**, 952-962.
7. T. Darden, D. York and L. Pedersen, *J. Chem. Phys.*, 1993, **98**, 10089-10092.
8. M. Parrinello and A. Rahman, *J. Appl. Phys.*, 1981, **52**, 7182-7190.
9. S. Páll, M. J. Abraham, C. Kutzner, B. Hess and E. Lindahl, *J. Chem. Phys.*, 2015, **70**, 139.
10. B. Ma, S. Kumar, C. J. Tsai and R. Nussinov, *Protein Eng.*, 1999, **12**, 713-720.
11. Schrodinger, LLC, unpublished work.